Manufacturing Letters 40 (2024) 58–64

Contents lists available at ScienceDirect

Manufacturing Letters

journal homepage: www.elsevier.com/locate/mfglet

Letters

Forest hardening and Hirth lock during grinding of copper evidenced by MD simulations

Ashwani Pratap [a,b], Nirmal Kumar Katiyar [c,d], Pengfei Fan [c], Saurav Goel [c,e,*], Suhas S Joshi [a,f]

[a] Indian Institute of Technology Bombay, Powai 400076, India
[b] ZEEKO KK, Japan
[c] London South Bank University, 103 Borough Road, London SE1 0AA, UK
[d] Amity Institute of Applied Sciences, Amity University Noida 201303, India
[e] University of Petroleum and Energy Studies, Dehradun 248007, India
[f] Indian Institute of Technology Indore, Simrol, Madhya Pradesh 453552, India

ARTICLE INFO

Article history:
Received 30 July 2023
Received in revised form 1 March 2024
Accepted 5 March 2024
Available online 6 March 2024

Keywords:
Dislocation
Molecular Dynamics
Copper
Internal stresses

ABSTRACT

Through the use of molecular dynamics (MD) simulation, grinding process of a single crystal copper with two scratch configurations (i) near spacing (NS) between adjacent scratches, and (ii) far spacing (FS) between adjacent scratches were simulated and compared to the control sample i.e., a single scratch (SS). FS configuration revealed the highest material removal, whereas NS configuration showed that the material removal is affected by various types of defects in the sub-surface which include FCC intrinsic stacking fault, a coherent twin boundary next to an intrinsic stacking fault and two adjacent intrinsic stacking faults. The formation of a Stair-rod 1/6 ⟨1 1 0⟩ due to the reaction between two Shockley partial dislocations 1/6 ⟨1 1 2⟩ was seen as a distinct feature of the NS configuration which forms the onset of hardening.

1. Introduction

Grinding of metallic substrates is the primary manufacturing operation followed in industries to shape and design various engineering components. The material removal mechanism during grinding is a complex process, and many models and theories have been presented by various researchers over several decades [1]. Many parameters can affect the material removal mechanism during the grinding process, such as the cutting parameters (cutting speed, work feed, depth of cut), cutting fluid types and their mode of delivery, and the abrasive grits particularly their distribution, spacing and bonding with the grinding wheel. The plastic flow occurring during the grinding of metallic components results from the movement and propagation of dislocations in the ground material. Unlike, single grit scratching, the movement of dislocations during grinding can intersect each other since the two simultaneously positioned grits can enter the workpiece consecutively or parallelly, directly affecting the subsurface dislocation interactions and leading to dislocation repelling or dislocation pinning and Lomer lock formation. Surprisingly, this hypothesis has never been proven experimentally as a real-time examination of these events during a high-strain rate operation such as grinding is difficult. This became a key motivation in undertaking the atomic simulation approach for this work and to understand the mechanics of material removal to compare the differences in adjacent scratches when they are near or sufficiently distanced. Such an understanding is vital to improve the design of the grinding wheel to execute energy efficient cutting processes.

In the past, Opoz *et al.* [2] researched single-grit grinding and defined the material removal mechanism by characterising pile-up and chip formation. They concluded that the material pile-up increases with the wearing out of the grit, and the pile-up phenomena were extremely high at the exit side of the scratch. Alhafez et al. [3] conducted multiple scratching on a bcc Fe crystal. The follow up scratch was carried out on top of the existing scratch area, with incremental scratch depth of 2 nm. It was established that the plastic zone in the 2-cycle scratch was more compact but contains more dislocations since during the second cycle the tip interacted with the previously formed dislocations. Zhang *et al.* [4] performed the MD simulation on double-grit scratching of copper to understand the interaction effect of two grits cutting adjacently. They suggested that two distinct high-quality parallel grooves could be obtained on the work surface regardless of the feed, depth and crystal orientation. Sharma *et al.* [5] performed a nanometric cut-

* Corresponding author at: London South Bank University, 103 Borough Road, London SE1 0AA, UK.
E-mail address: GoeLs@Lsbu.ac.uk (S. Goel).

https://doi.org/10.1016/j.mfglet.2024.03.002

ting simulation of copper using MD simulation and asserted that the propagation of dislocations is prevalent in the ⟨1 1 0⟩ slip on all the crystal orientations. Zhang et al. [6] compiled an extensive literature on interaction of dislocations and their effect on material response. It was established that the dislocations may either penetrate the interfaces by inducing steps into the interfaces or dissociate within the interfaces, depending on the type and orientation of the interface as well as the applied strain.

Extant literature reveals that a myriad of research efforts has been undertaken to understand the material removal mechanism during grinding of metallic materials such as copper, and also on studying the dislocation interactions. However, product-oriented experimental research has mostly remained focused on optimising the cutting parameters. Analysis of deeper aspects relating to pile-up and elastic recovery after grinding is quite limited. There is a clear knowledge gap concerning what happens when the spacing between the two cutting grits on the grinding tool is varied and what optimal spacing will yield an improved material removal process. This work addresses this question by embracing the use of MD simulation and clarifying the influence of grit spacing during the material removal process. Although, copper was chosen as a sample material for this study, the proposed theory is well applicable to explain the influence of grit spacing for a wide range of metallic materials. The emphasis of the study is not to match the experimental macro scale rather to reveal the phenomena of material removal and dislocation with adjacent grits processing the workpiece considering a nano scale simulation.

2. Method

A schematic MD model emulating the grinding process adopted from previous MD studies is shown in Fig. 1 [7–9] and details of the simulation was provided in Table 1. The MD simulation model adopted in this study consists of a monocrystalline copper workpiece (face-centred cubic (FCC) structure with a lattice constant of 0.36 nm) and two spherical diamond grits (each grit with a diameter of about 8.188 nm containing 47,146 carbon atoms). The size of the copper workpiece was 30 × 20 × 50 nm (in X, Y and Z directions, respectively as shown in Fig. 1-b containing 2.59 million atoms). Cutting depth was taken as 2 nm. Size effect is said to prevail when depth of cut is less than 1/3rd of the cutting-edge radius. A depth of cut of 2 nm (which is 1/2 of the cutting-edge radius 4 nm) was chosen for cutting to ensure dominant shearing. Ploughing will be present but the cutting mode will be shearing dominant which is always preferable. The cutting region was modelled as Newton-type atoms (LAMMPS NVE dynamics) and the outer periphery was fixed while an intermittent

Table 1
Process variables and details of the MD simulation model.

Copper workpiece dimensions	30 nm × 20 nm × 50 nm (X, Y and Z direction)
Depth of cut	2 nm
Workpiece cut surface and cutting direction	(0 1 0) and ⟨1 0 0⟩
Cutting tool	Spherical shaped with diameter of 8.188 nm
Total tool travel distance	16 nm (6 nm free travel)
Velocity of the tool	200 m/s = 0.2 nm/ps
Total simulation time	16 nm/0.2 nm/ps = 80 ps
MD Timestep	1 fs = 1 × 10^{-3} ps
Total run timesteps	80/0.001 = 80,000

langevin thermostat was provided to dissipate the heat which in experiments is carried away by air and cutting chips. This methodology has widely been followed over the past years including our previous works [10–12]. The force field (potential function) scheme used in this study (see Table 2**)** was that of a mixed/hybrid type since there is no single many body potential available to describe the interactions between carbon and copper atoms.

A small volume of copper material in the cutting zone (dimensions 1 nm × 1 nm × 1 nm) was identified for the purpose of stress and temperature computations. Scalar stress was obtained by converting the atomic stress tensor information obtained from LAMMPS (stress/atom) by dividing the volume of this atomic region with the total atomic stress. The instantaneous stress fluctuations were quite high, so the information of stress and temperature was time averaged using LAMMPS ave/atom command at every 10 steps repeated over 500 steps at a frequency of 5000 steps. For example, if Nevery = 10, Nrepeat = 500 and Nfreq = 5000, then values on timesteps 0, 10, 20, 30, 40, 50, 60. . . . . .4970, 4980, 4990. . ..until 5000 will be used to compute the final average on time step 5000.

The three cases of simulation (**see** Fig. 1a) involved (i) a single scratch (SS) simulation where a single diamond grit was moved across the work surface along the X-direction (ii) two adjacent diamond grits kept in near vicinity having a centre-to-centre distance of 9 nm, or the edge to edge spacing of 1 nm. This simulation setup was labelled as near scratch (NS) configuration hereafter, and (iii) the far scratch (FS) simulation where the two diamond grits had the centre-to-centre distance of 22 nm or edge-to-edge spacing of 14 nm. These values were decided based on the preliminary observations. For 14 nm of edge-edge spacing, there were no interactions observed in the cutting regions of both the grits whereas edge-edge to spacing 1 nm showed strong interactions in the cutting regions. For all three configurations, a velocity-controlled

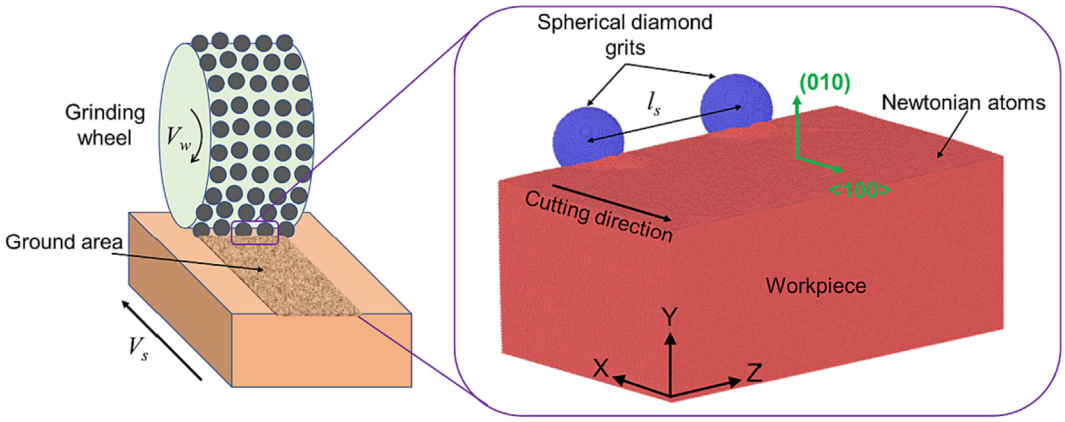

Fig. 1. MD simulation model to emulate the grinding process. The distance l_s was varied during the simulations.

Table 2
Scheme of the force field (potential energy function) adopted in this study to perform the MD simulations.

Interaction type	Potential used
Cu-Cu interactions (Workpiece atoms)	An embedded-atom-method (EAM) [13] with parameters used in their study by Goel *et al.* [14]
C–C interactions (Tool atoms)	Tersoff [15]
Cu-C interactions (Workpiece-tool atoms)	Morse potential adopted from Goel *et al.* [16] D (eV) = 0.087, A ($Å^{-1}$) = 1.7 and r_0 (Å) = 2.05

scratching was performed using the cutting velocity of 200 m/s. The cutting length was about 10 nm on the (010) plane along the ⟨100⟩ X-direction.

Four parameters were used to analyze the data, namely pile-up area (PA), groove area (GA), effective material removal (EMR) and groove depth, to measure the material removal effectiveness of the scratching process under different configurations. Pile-up area (PA) refers to the area at the edges of the scratch (above the top surface of the workpiece) where work material does not form chips and remains stick to the workpiece. The groove area (GA) represents the area of the groove formed during the scratching of the workpiece surface. Effective material removal is defined as the ratio of groove area to the summation of groove area and pile-up area, which is expressed as:

$$EMR = \frac{GA}{GA + PA} \quad (1)$$

3. Results and discussion

3.1. Material removal mechanism and structural evolution

Typical scratch profiles generated during three cutting configurations (SS, NS, FS) are shown in Fig. 2(a). It could be seen that the material removal during multi-grit cutting is far more complex than during the single grit cutting process. It can also be noticed that the material pile-up combines and accumulates in the NS configuration. As for the FS, two scratches look visually distinct with no overlap in the pile-up. At the macroscopic level, mechanical processing performance is generally measured in terms of material removal and surface features. The estimates of pile-up area (PA) and groove area (GA) in a typical 2D view of the scratch are shown in Fig. 2(b). Also, the pile-up area (PA) and groove area (GA) for the NS and FS configurations were scaled down by a factor of 0.5 to obtain the material removal strength per diamond grit to have a direct comparison with the SS configuration. The variations in PA, GA and EMR in relation to the scratch configuration is shown in Fig. 2(b). It could be seen that the pile-up per tool grit was the highest for SS and showed a decreasing trend for NS and FS.

Scratch force in the X-direction and normal force in the Y-direction extracted from the scratching process are shown in Fig. 2(c) and 2(d). Before the commencement of cutting, there was a large degree of workpiece compression, and once the material starts to flow on the tool's rake face, the compression is dominated by the shear, and this stage represents a steady-state cutting process. For the cutting depth of 2 nm and grit diameter of 8 nm,

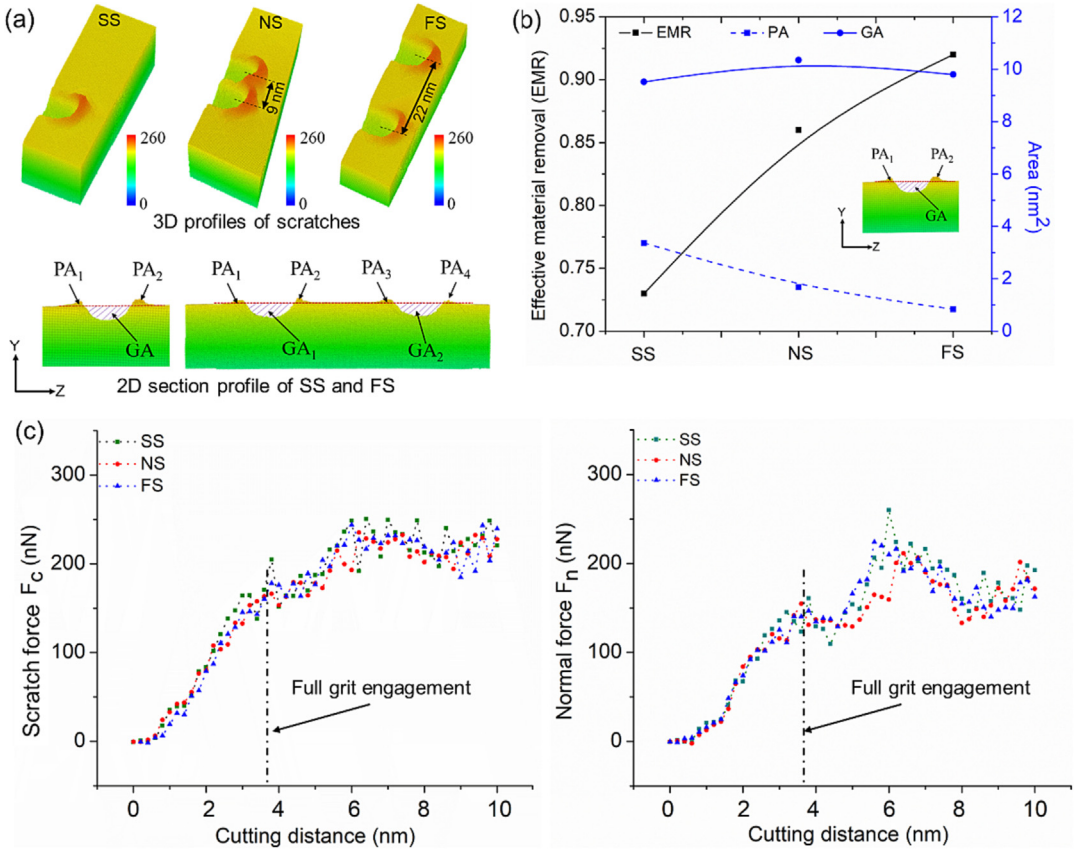

Fig. 2. (a) 3-dimensional topography of single scratch (SS), near scratch (NS), and far scratch (FS) (b) effective material removal (EMR), pile-up area, and groove area for SS, NS and FS, (c) scratch and (d) normal force evolution during SS, NS, FS.

the grit was seen to achieve steady-state cutting after a cutting distance of about 3.57 nm. Normal forces were a bit lower for NS case due to overlapping material removal. Normal force fluctuated more as compared to the scratching force. This fluctuation is associated with the elastic recovery and pile up material along the path. Fluctuation in force along the cutting path represents the unsteady nature of the tool-workpiece contact which will be directly responsible for generation of surface waviness.

The change in atomic structure and the movement of dislocations can be good indicators to obtain information about the quality of material removal across different scratch configurations. The single crystal copper has FCC crystal structure which has 12 slip systems. Under the effect of cutting stress, few stacking fault becomes apparent as a consequence of the FCC copper transforming to defect structures resembling as hcp structures with 2, 3 and 4 layers of hcp like configurations. The growth of defects under dif-

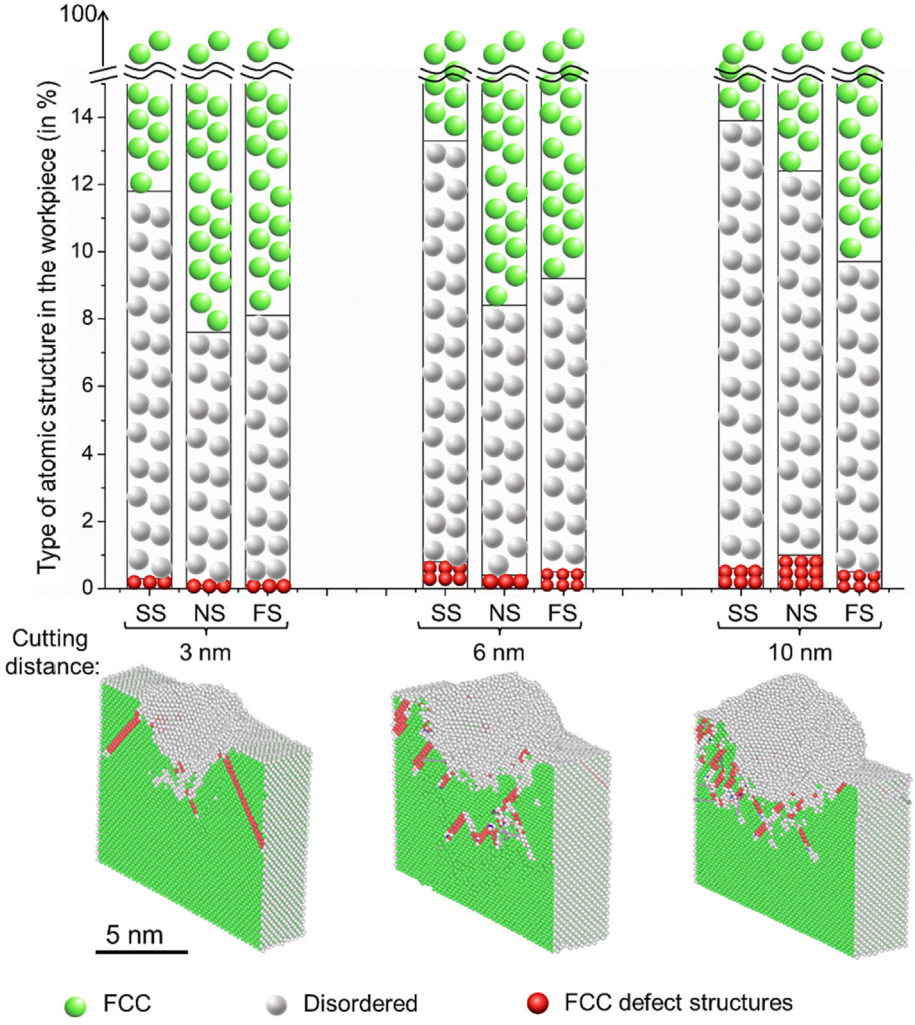

Fig. 3. Evolution of material defects during the scratching process in the three test cases simulated in this work.

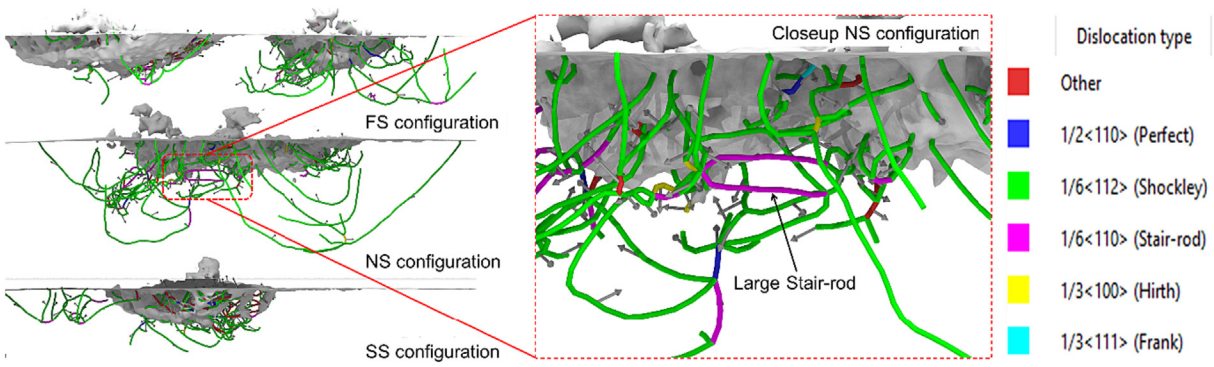

Fig. 4. Change in sub-surface dislocation behaviour SS, NS and FS configurations.

ferent cutting configurations (SS, NS and FS) at different instances of cutting lengths (3 nm, 6 nm and 10 nm) are shown in Fig. 3. Another type of atomic structure in the workpiece could be seen, and the percentage of different types of structures was calculated as equal number of atoms showing a specific type of atomic structure / total number of atoms. After the cutting process attains a steady state, the largest number of stacking faults can be seen in the NS configuration. These faults were of type FCC intrinsic stacking faults (2 hcp layered like defect structure), a coherent twin boundary next to an intrinsic stacking fault (3 hcp layered like defect structure) and two adjacent intrinsic stacking faults (4 hcp layered defect structure). It means that the lattice orientations on the two sides of a 3-layer fault were different, but the lattice orientation was the same on either side of 2- or 4-hcp resembling layers. The effective material removal during the SS configuration was the lowest and highest for the FS configuration. EMR of NS configuration was higher than that of SS and lower than that of the FS, because the material overlapping between the two grits gets removed during cutting.

3.2. Surface dislocations and elastic recovery

Fig. 4 shows various types of dislocation structures in the sub-surface of the scratched area. In FCC materials, Shockley dislocations are the most prevalent type of dislocations as were seen during the simulated cases in this work. Two common dislocations in an FCC structure are the Hirth dislocation which can result from reactions between Shockley dislocations as $1/6[\bar{1}\,\bar{2}\,1] + 1/6[\bar{1}\,2\,\bar{1}] = 1/3[\bar{1}\,00]$ and Frank dislocation which can result from reactions of Stair-rod and Shockley, e.g., $1/6[011] + 1/6[211] = 1/3[111]$. Hirth dislocations are referred to as Hirth locks [17], and Frank dislocations are known as Lomer–Cottrell (LC) locks. A Lomer lock is a type of sessile dislocation that acts as a pinning point in forest hardening. When dislocations move under tensile stress, their stress fields interact. As the elastic strain energy is proportional to the square of the local strain, it is energetically favourable for the stress fields to configure themselves to minimise this strain. It could be observed that the area density of dislocations increased along the cutting length. Copper with the FCC structure has 12 non-equivalent partial dislocation slip systems $\langle 1\,1\,0\rangle/2\{1\,1\,1\}$. However, not all these slip systems are operative during scratching. We can convert the applied shear (scratching) stress to each slip system based on tensor rotation. The slip systems with the maximum conversion factors (analogous to the Schmid factor) are operative. We saw that the (0 1 0) scratching has eight most likely operative slip systems $[1\,0\,1]/2\_(\bar{1}\,1\,1)$, $[0\,\bar{1}\,1]/2\_(\bar{1}\,1\,1)$, $[1\,0\,1]/2\_(1\,1\,\bar{1})$, $[0\,1\,1]/2\_(1\,1\,\bar{1})$, $[0\,1\,1]/2\_(\bar{1}\,1\,\bar{1})$, $[1\,0\,\bar{1}]/2\_(\bar{1}\,1\,\bar{1})$, $[0\,\bar{1}\,1]/2\_(1\,1\,1)$, $[\bar{1}\,0\,1]/2\_(1\,1\,1)$ with a conversion factor of 0.41 [18]. During scratching in the FS configuration, the dislocations in the sub-surface under the two grits showed no interaction or overlap. From the comparison of three configurations and a close up of the NS configuration, as shown in Fig. 4, a large stair-rod forming as a result of the reaction between two Shockley's can be seen. This stair rod forming the Hirth lock led to work hardening when two scratches are nearly distanced. This limits the movement of dislocations at the outer boundaries of the two scratches. It explains the hardening of pile-up material during NS configuration and suggests that the dislocation pinning during the grinding of copper restricts the free mobility of Shockley dislocations. Overall, it was found that the Shockley dislocation acts as a transporter of plasticity under the sub-surface which appears to be straightforward during SS and FS configurations, but it meets a competing force due to the Hirth lock during the NS configuration.

Elastic recovery of scratched grooves could be calculated using the relation between the theoretical scratch geometry (based on grit and workpiece interaction area) and the measured scratch

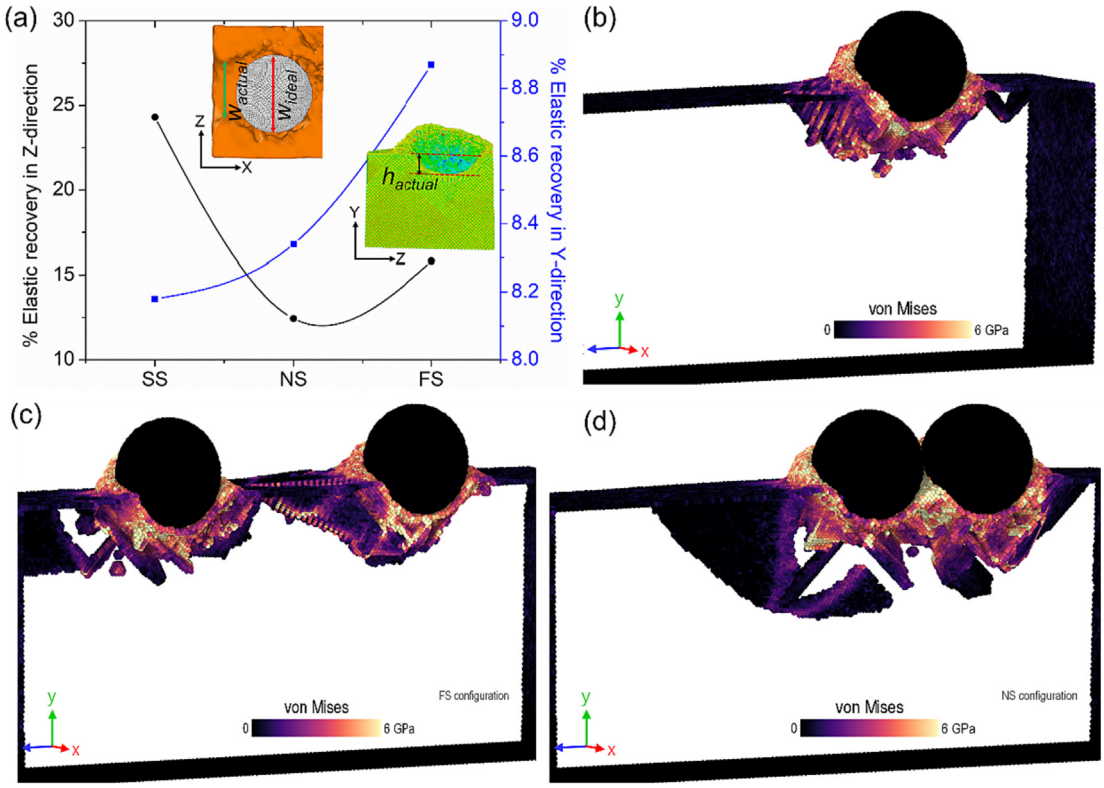

Fig. 5. (a) Variation in the elastic recovery and (b), (c), (d) stress distribution for SS, FS and NS respectively.

geometry. However, the measured width and depth are always less than the theoretical measure due to the elastic recovery of the workpiece. The percentage elastic recovery can be calculated as:

$$\%elasticrecoveryinZdirection = \frac{w_{ideal} - w_{actual}}{w_{ideal}} \times 100 \quad (2)$$

$$\%elasticrecoveryinYdirection = \frac{h_{ideal} - h_{actual}}{h_{ideal}} \times 100 \quad (3)$$

The percentage elastic recovery in the *Z*-direction (scratch width direction) and *Y*-direction (scratch depth direction) for different configurations can also be seen in Fig. 5(a). In the prima facie, it is evident that the elastic recovery is more prominent in the *Z*-direction as compared to the *Y*-direction [19]. It can be explained by the variable stress distribution along the contact zone, shown in Fig. 5 (b), (c), (d). The cutting stress varies along the cutting-edge radius, being maximum at the center, and therefore the material at the centre is compressed to the maximum possible extent compared to the material sideways. Therefore, the work material at the valley of the scratch showed a lower amount of elastic recovery. Secondly, the elastic recovery along the Y-direction does not differ significantly during SS, NS and FS and its extent was just about 8 % to 9 %. The extent of elastic recovery in the *Z*-direction was seen to be higher and significantly dependent on the scratch configuration. The highest elastic recovery of 23.4 % could be observed for the SS configuration as there is no dislocation pinning and restriction on material flow. The elastic recovery was lowest at 12.44 % for the NS configuration, which occurred due to the forest hardening due to the formation of Hirth locks and L-C locks.

4. Conclusions

This work addresses an important research gap in understanding the material removal mechanism of abrasive cutting tools such as grinding. A molecular dynamics study was performed to observe the interaction between various dislocations when two closely spaced abrasive grits were compared with a sufficiently distanced grits during scratching of copper. Following conclusions were drawn from the outcomes:

- During single grit scratching, a Shockley dislocation 1/6 ⟨1 1 2⟩ serves the role of transporting the plasticity but in scenario's when two adjacent grits scratches a surface, the two Shockley can react to form a stair rod which results in a Hirth lock leading to strain accumulation and work hardening. Too close positioning of abrasive grits on the grinding wheel would therefore lead to the generation of hardened surface and difficulty in the materials processing due to restricted dislocation movement.
- The elastic recovery of material was seen higher in the transverse direction as compared to the normal direction, caused by variable stresses across the cutting-edge radius. The elastic recovery amount was higher if the cutting grits are sufficiently distance apart, again due to the lower strength of dislocation pinning.
- Average forces on a grit during scratching was almost similar in case of single scratch and far scratch configuration, however, a bit lower due to overlapping material removal in case when two grits were positioned in very near domain.

The present study is limited to observation of dislocation behaviour during dry scratching. However, most of the grinding and cutting processes are carried out in the presence of cutting fluids in order to achieve better surface finish and lower tool wear. Molecular dynamics simulation with cutting fluids similar to the recent efforts may be a good follow up work [20], and further studies should be carried out to observe the effects of cutting fluids on pile-up and dislocation interaction during multiple scratching. Secondly, the effective material removal (EMR) parameter presented in this study considers only ploughing and shearing, whereas neglects the effect of elastic deflection. However, it is well known that elastic deflection can be quite significant during small scale removal processes. Therefore, a modified parameter (in place of EMR) should be established in the future to accommodate the effect of elastic deflection.

CRediT authorship contribution statement

Ashwani Pratap: Conceptualization, Formal analysis, Investigation, Methodology, Writing – original draft. **Nirmal Kumar Katiyar:** Data curation, Formal analysis, Software, Writing – review & editing. **Pengfei Fan:** Methodology, Validation, software, Writing – review & editing. **Saurav Goel:** Conceptualization, software, Funding acquisition, Project administration, Writing – review & editing. **Suhas S Joshi:** Conceptualization, Supervision, Funding acquisition, Project administration, Writing – review & editing.

Declaration of competing interest

The authors declare that they have no known competing financial interests or personal relationships that could have appeared to influence the work reported in this paper.

Acknowledgement

SG would like to acknowledge the financial support provided by the UKRI via Grants No. EP/S036180/1 and EP/T024607/1, Hubert Curien Partnership Programme from the British Counsil and the International exchange Cost Share award by the Royal Society (IEC\NSFC\223536). Additionally, we are grateful to be granted the access of various HPC resources including the Isambard Bristol, UK supercomputing service as well as Kittrick (LSBU, UK), Magus2 (Shiv Nadar University, India) and Param Ishan (IIT Guwahati, India).

Data statement

All data underpinning this publication are openly available from the University of Strathclyde Knowledge Base.

References

[1] Pan Y, Zhou P, Yan Y, Agrawal A, Wang Y, Guo D, et al. 2021, "new insights into the methods for predicting ground surface roughness in the age of digitalisation". Precis Eng November 2020;67:393–418.
[2] Öpöz TT, Chen X. Experimental study on single grit grinding of inconel 718. Proc Inst Mech Eng Part B J Eng Manuf 2015;229(5):713–26.
[3] Alabd Alhafez I, Kopnarski M, Urbassek HM. Multiple scratching: an atomistic study. Tribol Lett 2023;71(2):1–9.
[4] Zhang P, Zhao H, Shi C, Zhang L, Huang H, Ren L. Influence of double-tip scratch and single-tip scratch on Nano-scratching process via molecular dynamics simulation. Appl Surf Sci 2013;280(September):751–6.
[5] Sharma A, Datta D, Balasubramaniam R. Molecular dynamics simulation to investigate the orientation effects on nanoscale cutting of single crystal copper. Comput Mater Sci 2018;153(April):241–50.
[6] Zhang Z, Shao C, Wang S, Luo X, Zheng K, Urbassek HM. Interaction of dislocations and interfaces in crystalline heterostructures: a review of atomistic studies. Crystals 2019;9(11).
[7] Pan Y, Zhou P, Yan Y, Agrawal A, Wang Y, Guo D, et al. New insights into the methods for predicting ground surface roughness in the age of digitalisation. Precis Eng 2021;67:393–418.
[8] Chavoshi SZ, Xu S, Goel S. Addressing the discrepancy of finding the equilibrium melting point of silicon using molecular dynamics simulations. Proc R Soc A 2017;473:20170084.
[9] Faisal NH, Prathuru AK, Goel S, Ahmed R, Droubi MG, Beake BD, et al. Cyclic nanoindentation and Nano-impact fatigue mechanisms of functionally graded TiN/TiNi film. Shape Mem Superelasticity 2017;3(2):149–67.

[10] Goel S, Kovalchenko A, Stukowski A, Cross G. Influence of microstructure on the cutting behaviour of silicon. Acta Mater 2016;105:464–78.
[11] Kumar D, Goel S, Gosvami NN, Jain J. Towards an improved understanding of plasticity, friction and Wear mechanisms in precipitate containing AZ91 mg alloy. Materialia 2020;10:1–36.
[12] Fan P, Katiyar NK, Zhou X, Goel S. Uniaxial pulling and Nano-scratching of a newly synthesized high entropy alloy. APL Mater 2022;10(11).
[13] Foiles SM, Baskes MI, Daw MS. Embedded-atom-method functions for the Fcc metals Cu, Ag, Au, Ni, Pd, Pt, and their alloys. Phys Rev B 1986;33 (12):7983–91.
[14] Goel S, Faisal NH, Ratia V, Agrawal A, Stukowski A. Atomistic investigation on the structure-property relationship during thermal spray nanoparticle impact. Comput Mater Sci 2014;84:163–74.
[15] Tersoff J. Modeling solid-state chemistry: interatomic potentials for multicomponent systems. Phys Rev B 1989;39(8):5566–8.
[16] Goel S, Luo X, Agrawal A, Reuben RL. Diamond machining of silicon: a review of advances in molecular dynamics simulation. Int J Mach Tools Manuf 2015;88:131–64.
[17] Paulauskas T, Buurma C, Colegrove E, Stafford B, Guo Z, Chan MKY, et al. Atomic scale study of polar lomer-Cottrell and hirth lock dislocation cores in CdTe. Acta Crystallogr Sect A Found Adv 2014;70(6):524–31.
[18] Bulatov V, Abraham FF, Kubin L, Devincre B, Yip S. Connecting atomistic and mesoscale simulations of crystal plasticity. Nature 1998;391(6668):669–72.
[19] Pratap A, Divse V, Goel S, Joshi SS. Understanding the surface generation mechanism during micro-scratching of ti-6Al-4V. J Manuf Process 2022;82:543–58.
[20] Stephan S, Schmitt S, Hasse H, Urbassek HM. Molecular dynamics simulation of the stribeck curve: boundary lubrication, mixed lubrication, and hydrodynamic lubrication on the atomistic level. Friction 2023;11 (12):2342–66.